Lasers in Manufacturing Conference 2019

Laser doping for 4H-SiC power-device fabrication with laser pulse-duration controller

Toshifumi Kikuchi[a,b*], Kaname Imokawa[a,b], Akihiro Ikeda[c], Daisuke Nakamura[a], Tanemasa Asano[a], Hiroshi Ikenoue[a,b]

[a]*Grad. Sch. ISEE. Kyushu Univ.,*
[b]*Dept. of Gigaphoton Next GLP, Kyushu Univ.,*
[a,b]*744 Motooka, Nishi-ku, Fukuoka 819-0395, Japan*
[c]*Sojo Univ., 34-22-1 Ikeda, Nishi-ku, Kumamoto 860-0082, Japan*

Abstract

We have investigated a KrF excimer laser doping method for high-concentration, low-temperature doping of 4H-SiC. We reported that heavy N or Al doping of the 4H-SiC can be achieved by laser ablation of thin source films (SiN_x or Al) formed on the SiC substrate. Recently, we developed a laser doping system capable of processing the entire SiC wafer with high productivity for manufacturing systems. In this system, a gas supply nozzle for ambient environment control was installed to prevent oxidation of the SiC surface, achieving the same oxidation-suppression effect as a vacuum chamber. Furthermore, the system contains an optical pulse stretcher that lowers the laser peak pulse and stretches the pulse width. By using the KrF excimer laser doping system, we achieved high concentration and high throughput doping of 4H-SiC at low temperature and low contact resistance.

Keywords: laser doping, power device, semiconductor, excimer laser, 4H-SiC;

1. INTRODUCTION

4H-silicon carbide (4H-SiC) is a group IV semiconductor with a bandgap energy of 3.26 eV, and it is known as a promising material for high-power devices. It has several superior material properties, in particular, a dielectric breakdown field approximately 10 times larger than that of silicon (Si) [1−5]. Therefore, SiC devices have lower electric power losses than Si devices.

However, some issues must be overcome to fabricate SiC devices. One such issue is the difficulty of the doping process. Because SiC has a lower electron affinity than Si [6], upon SiC doping, a larger Schottky barrier is formed, and the contact resistance tends to be larger than that of Si [7−9]. Thus, heavy doping is necessary to form low-resistance contacts. Nitrogen and phosphorous have been widely studied as n-type dopants of SiC [1]. Hot ion implantation at a high temperature of approximately 600 °C and subsequent annealing at approximately 1700 °C are typically used to dope SiC [10−15]. However, the concentration limit of the dopants is in the order of $10^{20}/cm^3$[16]. The surface concentration is lower than the bulk concentration because the dopant diffuses very little, even at such high temperatures. Therefore, it is difficult to reduce the metal/SiC contact resistance and high-temperature annealing from 800 to 1000 °C is required for electrode formation to reduce the contact resistance due to alloying and defect generation at the metal/SiC interface [5]. These high-temperature processes degrade the crystallinity of the SiC by, for example, segregating C atoms from the SiC bulk [17−19]. Furthermore, the process integration is limited; for example, thinning of the SiC substrate is difficult. The process is performed under a vacuum equipment, and a huge vacuum chamber is required, leading to an increase in size and cost of the device.

* *Corresponding author. Tel.: +81-80-5536-6070;*
E-mail address: author@institute.xxx .

We have investigated a laser doping method for high-concentration, low-temperature doping and reported that heavy N or Al doping of 4H-SiC can be achieved by laser ablation of thin source films (SiN_x or Al) formed on the SiC substrate [20−26]. Recently, we have developed a laser doping method capable of processing the entire SiC wafer with high productivity for a manufacturing system. In this system, a gas supply nozzle for ambient environment control was installed to avoid oxidation of the SiC surface. With this gas supply nozzle, the same oxidation-suppression effect achieved by a vacuum chamber can be expected. Furthermore, the system contains an optical pulse stretcher (OPS) that lowers the laser peak pulse and can stretch the pulse width. The effects of the pulse width on laser ablation can be observed with the OPS. In this paper, we report the influence of the laser pulse width when the excimer laser is irradiated on the 4H-SiC substrate. Furthermore, by using a nozzle, the same effects of a vacuum can be achieved. Finally, we will discuss the contact resistance during electrode formation for N-doped regions formed using this laser doping system.

2. EXPERIMENTAL

2.1. Experimental conditions

The sample structure was a SiN_x(100 nm)/n-type 4H-SiC(0001) substrate. The SiN_x film was deposited on the C-face of the SiC substrate by chemical vapor deposition. Figure 1 shows a schematic diagram of the laser irradiation system. Laser irradiation was performed by a KrF excimer laser (Gigaphoton Inc., wavelength: 248 nm. Pulse duration: 15 ns, full width at half-maximum). Figure 2 shows a schematic diagram of the sample structure and laser doping procedure. Laser irradiation of the sample was performed in Ar ambient by using a gas supply nozzle. The nozzle is very small (approximately 75 mm × 75 mm × 80 mm) and oxidation of the sample surface can be effectively suppressed. The pulse width (FWHM) of the laser beam was changed from 15 to 30 ns with the OPS. The laser peak energy was approximately half. The OPS will be described in detail in Section 2.2.The laser beam size on the sample surface was 300 µm × 400 µm, the irradiation fluence ranged from 2.0 to 3.2 J/cm^2, the laser was operated at 100 Hz, and the sample was scanned at rates of between 2 and 8 mm/s along the short-axis direction of the laser beam. Scan speeds of 2, 4, and 8 mm/s correspond to 15, 10, and 5 shots/loc., respectively. After irradiation, the non-irradiated area of the SiN_x films was removed by immersing the sample in a phosphorous acid solution at 150 °C for 25 min.

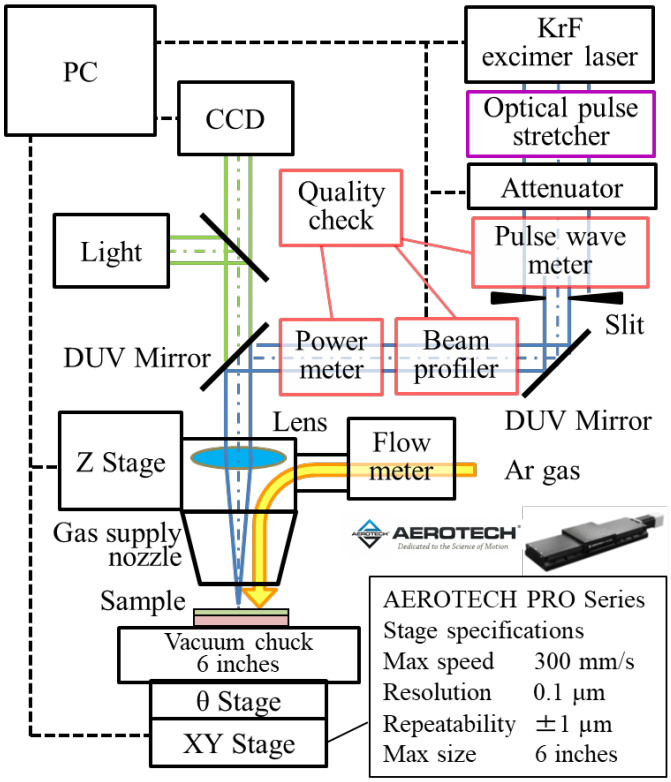

Fig. 1. Schematic of the laser irradiation system.

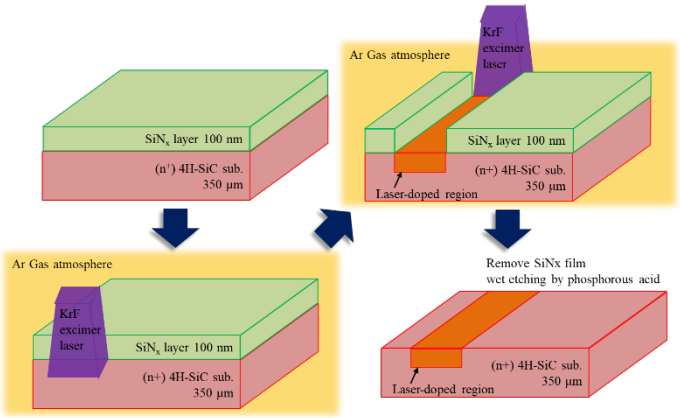

Fig. 2. Sample structure and laser doping procedure.

2.2. Optical pulse stretcher (OPS)

An OPS is a system that uses optical delay to extend the pulse width. A schematic of the OPS is shown in Figure 3. As shown in Figure 4, the pulse width of the KrF excimer laser is 15 ns. The pulse width is extended to 30 ns by inducing an optical path delay of 7 m. Furthermore, it is possible to extend the pulse width by adding OPS 4 m after OPS 7 m. In this paper, we will report the results obtained using the OPS 7 m.

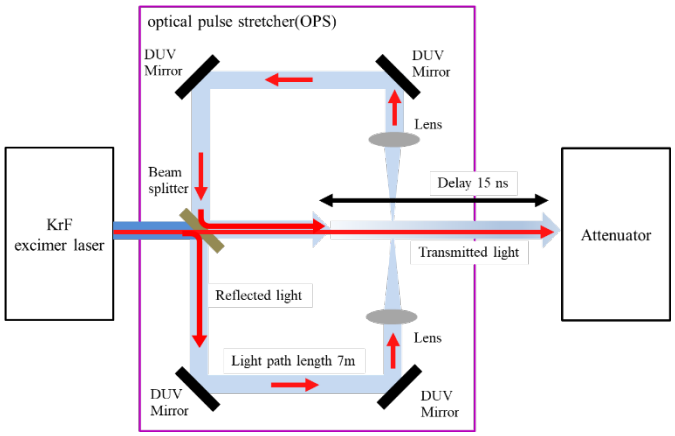

Fig. 3. Simplified optical diagram of optical pulse stretcher.

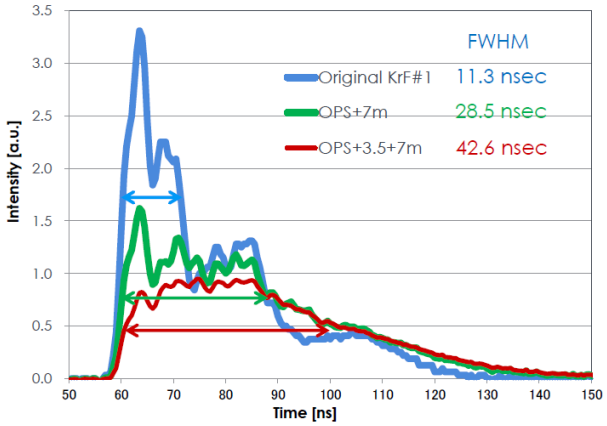

Fig. 4. Laser pulse waveform without OPS, with OPS+7 m and with OPS+3.5 m+7 m

2.3. Gas supply nozzle

Figure 5 shows a simplified view of the gas supply nozzle. The nozzle was supplied with a gas sprayed from the laser irradiation port and a shielding gas sprayed around the irradiation port. The distance between the sample and the nozzle was approximately 1 mm. A Z-stage for focusing was used for adjusting the position of the nozzle. The total flow rate of Ar gas was 2 L/min.

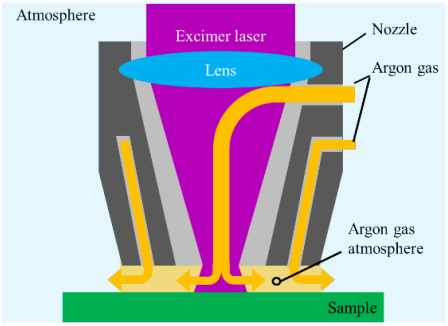

Fig. 5. Simplified view of the gas supply nozzle

3. RESULTS AND DISCUSSION

Figure 6 shows the current–voltage (*I–V*) characteristics of the surface after irradiation in vacuum (a) and Ar ambient and atmosphere (b). Figure 5(a) is taken from a previous report on irradiation in vacuum [26] where the fluence was set to 2.0 J/cm^2 and the number of shots to 10. The *I-V* plot obtained clearly shows ohmic linearity characteristics. The results in figure 4(b) were obtained with a fluence of 2.2 J/cm^2 and 10 shots. For irradiation in atmosphere, the *I–V* curve is nonlinear while for irradiation in Ar ambient, ohmic characteristics with linearity are clearly obtained. A characteristic close to that in vacuum and Ar gas atmosphere was obtained. Therefore, the developed gas supply nozzle effectively prevented the oxidation of the SiC surface.

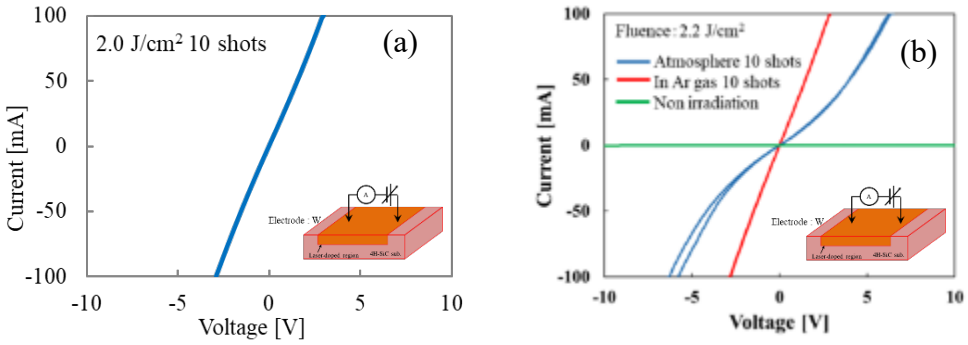

Fig. 6. (a) *I–V* characteristics of irradiation in vacuum from a previous report [26]. (2.0 J/cm^2, 10 shots)
(b) *I–V* characteristics of irradiation in Ar ambient and atmosphere. (2.2 J/cm^2, 10 shots)

Figure 7 shows the *I–V* characteristics of the surface with and without OPS. The low resistance values range from 2.2 to 3.0 J/cm^2 and from 2.1 to 2.3 J/cm^2 for irradiation with and without OPS, respectively. Thus, the use of the OPS causes the low resistance range to expand. The minimum resistance value shifts to the high fluence side. From this result, we conclude that the peak power of the laser is lowered by the OPS, and the electrical characteristics degradation induced by laser doping is reduced. Figure 8 shows the dependence of the resistance value on the number of irradiations for each fluence. The resistance value was 28.4 Ω for 5 shots, 28.4 Ω for 10 shots and 26.3 Ω for 15 shots when the irradiation condition was 2.4 J with OPS. It was confirmed that the resistance value decreased in a wide range of the number of irradiations. As the number of irradiations is increased, the resistance value increases and the SiC surface is ablated.

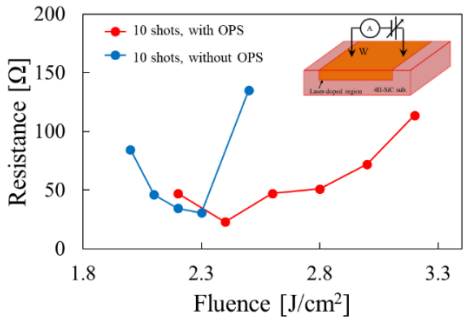

Fig. 7. Dependence of resistance on fluence and OPS. (Number of shots 10)

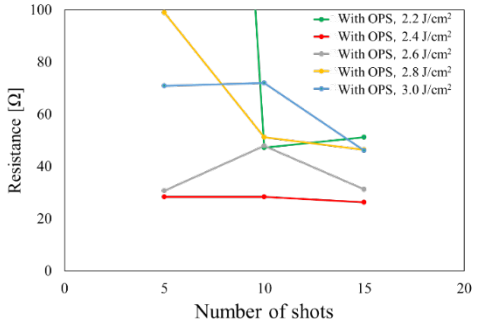

Fig. 8. Dependence of the resistance value on the number of irradiations for each fluence.

Figures 9 and 10 show the results of Raman analysis and the shape profile of the irradiation surface analysis with and without the OPS, respectively. The fluence was 2.4 J/cm^2 with OPS and 2.2 J/cm^2 without OPS. In the Raman analysis, the vertical axis represents the ratio of the near 780 cm^{-1} peak intensity of the 4H-SiC surface after irradiation to the unirradiated 4H-SiC substrate. Figure 9(a) shows the results of the Raman analysis without the OPS. The crystallinity was decreased to 70% after the laser irradiation. Figure 9(b) shows the results of the Raman analysis with the OPS. As shown in the figure, the crystallinity did not change.

Figure 10 shows a surface profile of the laser-irradiated surface, which was obtained by scanning the probing stylus over the irradiated area. Figure 10(a) shows the surface profile after irradiation without the OPS. The cross-sectional area of the surface bump after irradiation was approximately 3 μm^2. Figure 10(b) shows the surface profile after irradiation without the OPS. The cross-sectional area of the surface bump after irradiation was approximately 1.5 μm^2. Therefore, the OPS is effective in reducing the degradation of the crystallinity and improves bumps formation and the electron properties.

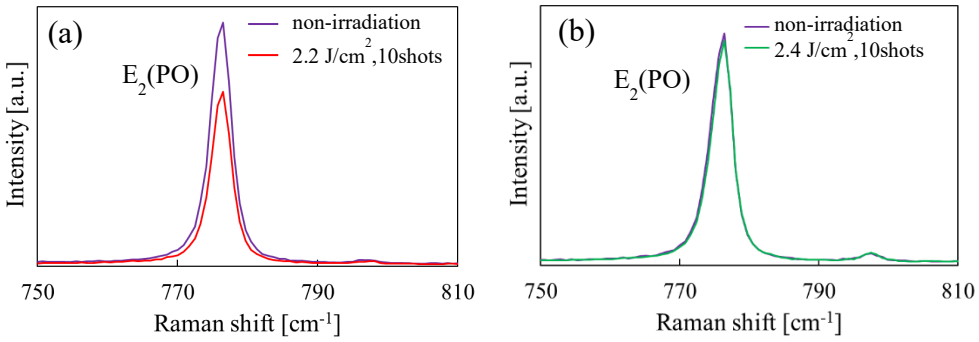

Fig. 9. (a) Raman spectrum of 4H-SiC at no irradiation area and the laser doping area without OPS. (2.2 J/cm^2, 10 shots)
(b) Raman spectrum of 4H-SiC at no irradiation area and the laser doping area with OPS. (2.4 J/cm^2, 10 shots)

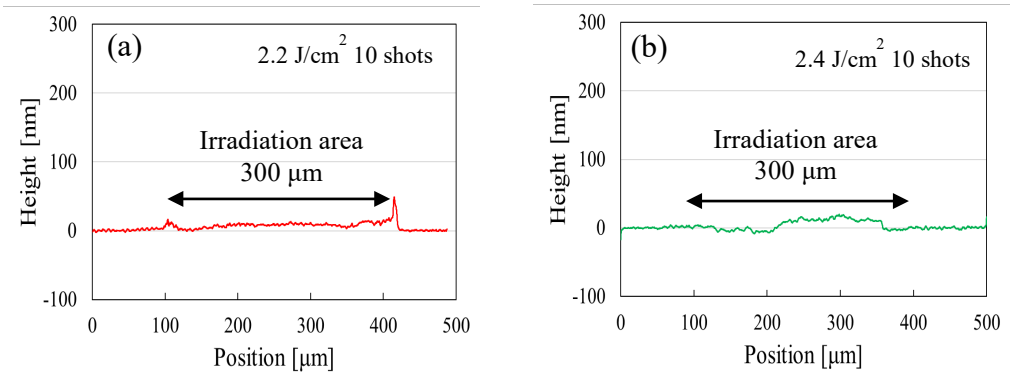

Fig. 10. (a) Surface bump of 4H-SiC laser doping area without OPS. (2.2 J/cm^2, 10 shots)
(b) Surface bump of 4H-SiC laser doping area with OPS. (2.4 J/cm^2, 10 shots)

Figure 11 shows the results of secondary ion mass spectrometry (SIMS) analysis of nitrogen after laser doping in Ar ambient (2.4 J/cm^2, 10 shots) with and without OPS. High-concentration nitrogen doping (at the 10^{21}/cm^3 level at the surface) was achieved in both conditions.

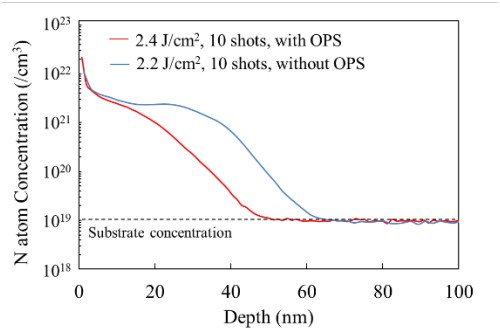

Fig. 11. SIMS depth profiles of N obtained from the sample irradiated with SIN_x film.

Figure 12 describes the contact resistance measurement method. Al/Ti electrodes with sizes ranging from 5 µm × 5 µm to 50 µm × 50 µm were deposited on the laser-doped region. When the electrode dimension d was much smaller than the SiC substrate thickness t, the bulk resistance R2 and Ni/SiC contact resistance R3 were considered constant. The contact resistance value can be calculated from the slopes of equations (1), (2), and (3).

The contact resistance value was calculated from the *I–V* measurement results. With a fluence of 2.2 J/cm^2 and 10 shots without the OPS, the contact resistance was 3.7 × 10-5 Ω·cm^3 without annealing. When the Al/Ti electrodes were annealed at 200 °C for 30 min, the contact resistance was 2.5 × 10-5 Ω·cm^3. Therefore, the annealing repaired the crystal defects. With the OPS, the contact resistance was 2.3 × 10-5 Ω·cm^3 without annealing. Thus, the OPS did not deteriorate the crystallinity, and few crystal defects were formed when the contact resistance decreased at room temperature.

$$R_M = R_1 + R_2 + R_3 \quad (1)$$

$$R_1 = \rho_C / d^2 \quad (2)$$

$$R_M = \rho_C / d^2 + R_2 + R_3 \quad (3)$$

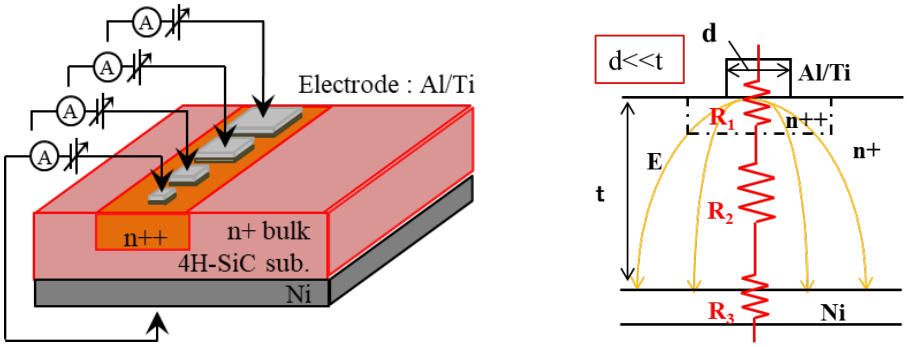

Fig. 12. Schematic diagram of a contact resistance measuring method (left) and measurement circuit diagram (right).

4. CONCLUSIONS

We proposed a method for low-temperature nitrogen doping of 4H-SiC(0001) induced by KrF excimer laser irradiation of a SiN_x film. The laser irradiation was performed using an Ar gas supply nozzle to avoid oxidation of the SiC surface. The gas supply nozzle was as effective as a vacuum in preventing SiC surface oxidation. The use of the OPS induced little degradation of the SiC crystallinity in the nitrogen-doped region. The deformation of the irradiated surface could also be suppressed. Therefore, high pulse energy adversely affects SiC. In terms of laser doping, we concluded that widening the pulse and lowering its peak energy improves the effectiveness. High-concentration nitrogen doping (at the 1021/cm3 level at the surface) can be achieved by laser ablation of the SiN_x film. With the OPS, the contact resistance between an Al/Ti electrode and the nitrogen-doped region is 2.3 × 10^{-5} Ω·cm^2 at room temperature. Therefore, if a back-side electrode for a Schottky barrier diode (SBD) or PiN diode is fabricated following this method, the power loss ratio of the contact resistance to the bulk resistance can be estimated to be 3.2 and 11.5% at substrate (0.02 Ω·cm) thicknesses of 350 and 100 µm, respectively. Then, a sufficiently small value of the backside contact resistance of SBD and PiN diodes can be obtained. In conclusion, low-temperature and high-concentration laser doping can be achieved by laser ablation of a SiN_x film on a 4H-SiC substrate. Furthermore, the use of the gas supply nozzle and the OPS stabilize the manufacturing process and reduces the cost of the system.

5. ACKNOWLEDGMENTS

We express our sincere thanks to the staff of Tamari industry for cooperating in the fabrication of the gas supply laser irradiation system.

6. REFERENCES

[1] D. Peters, R. Schorner, K. H. Holzlein, and P. Friedrichs, Appl. Phys. Lett. **71**, 2996 (1997).
[2] J. Spitz, M. R. Melloch, J. A. Cooper, and M. A. Capano, IEEE Electron Device Lett. **19**, 100 (1998).
[3] A. K. Agarwal, J. B. Casady, L. Rowland, S. Seshadri, R. Siergiej, W. Valek, and C. D. Brandt, IEEE Electron Device Lett. **18**, 518 (1997).
[4] A. Ishitani and Y. Kawana, Semicond. FPD World **4**, 63 (2008).
[5] Carl-Mikael Zetterling, Process Technology for Silicon Carbide Devices, INSPEC, London, **5** (2002).
[6] S. Yu. Davydov, Semiconductors 41 696 (2007).
[7] J. A. Cooper, M. R. Melloch, R. Singh, A. Agarwal, and J. W. Palmour, IEEE Trans. Electron Devices **49**, 658 (2002).
[8] P. Brosselard, A. P. Tomas, J. Hassan, N. Camara, X. Jorda, M. Vellvehi, P. Godignon, J. Millan, and J. P. Bergman, Semicond. Sci. Technol. **24**, 095004 (2009).
[9] K. Fujihira, S. Tamura, T. Kimoto, and H. Matsunami, IEEE Trans. Electron Devices **49**, 150 (2002).
[10] M. Laube, F. Schmid, G. Pensl, G. Wagner, M. Linnarsson, and M. Maier, J. Appl. Phys. **92**, 549 (2002).
[11] F. Schmid, M. Laube, G. Pensl, G. Wagner, and M. Maier, J. Appl. Phys. **91**, 9182 (2002).
[12] G. Pensl, T. Frank, M. Krieger, M. Laube, S. Reshanov, F. Schmid, and M. Weidner, Physica B **340–342**, 121 (2003).
[13] M. A. Capano, R. Santhakumar, R. Venugopal, M. R. Melloch, and J. A. Cooper, J. Electron. Mater. **29**, 210 (2000).
[14] L. Zhu, Z. Li, and T. P. Chow, J. Electron. Mater. **30**, 891 (2001).
[15] N. Yanagida, K. Ishibashi, S. Uchiumi, and T. Inada, Nucl. Instrum. Methods Phys. Res., Sect. B **257**, 203 (2007).
[16] Mulpuri V. Rao, Jesse B. Tucker, M. C. Ridgway, O. W. Holland, N. Papanicolaou, and J. Mittereder, Journal of Applied Physics **86**, 752 (1999).
[17] G. G. Jernigan, B. L. VanMil, J. Tedesco, J. G. Tischler, E. R. Glaser, A. Davidson, and P. M. Campbell, Nano Lett. **9**, 2605 (2009).
[18] I. Forbeaux, J. Themlin, and J. Debever, Surf. Sci. **442**, 9 (1999).
[19] T. Tsukamoto, M. Hirai, M. Kusaka, M. Iwami, T. Ozawa, T. Nagamura, and T. Nakata, Surf. Sci. **371**, 316 (1997).
[20] A. Ikeda, K. Nishi, H. Ikenoue, and T. Asano, Appl. Phys. Lett. **102**, 052104 (2013).
[21] K. Nishi, A. Ikeda, H. Ikenoue, and T. Asano, Jpn. J. Appl. Phys. **52**, 06GF02 (2013).
[22] K. Nishi, A. Ikeda, D. Marui, H. Ikenoue, and T. Asano, Mater. Sci. Forum **778–780**, 645 (2014).
[23] D. Marui, A. Ikeda, H. Ikenoue, and T. Asano, Jpn. J. Appl. Phys. **53**, 06JF03 (2014).
[24] Akihiro Ikeda, Daichi Marui, Hiroshi Ikenoue, and Tanemasa Asano, Jpn. J. Appl. Phys. **54** 04DP02 (2015)
[25] Akihiro Ikeda, Rikuho Sumina, Hiroshi Ikenoue, and Tanemasa Asano, Jpn. J. Appl. Phys. **55** 04ER07 (2016).
[26] R. Kojima, H. Ikenoue, M. Suwa, A. Ikeda, D. Nakamura, T. Asano and T. Okada Proc. SPIE **9738**, 973803. (April 06, 2016).